Disturbances in a power transmission system

M. L. Sachtjen, B. A. Carreras, and V. E. Lynch
Oak Ridge National Laboratory, Oak Ridge, Tennessee 37831
(Received 4 October 1999; revised manuscript received 7 January 2000)

A simple model for a power transmission system is presented. In this model, disturbances of all sizes may occur. They are randomly triggered and have the characteristic behavior of avalanches. A single parameter describes the scaling of the avalanche size. This parameter combines a measure of closeness to the maximum load, size of transferred loads during an overloading event, and connectivity of the system. The probability distribution function of the size of the disturbance has power-scaling range with the exponent close to -1.

PACS number(s): 05.40.−a, 05.45.−a

I. INTRODUCTION

Power transmission systems are complex systems. Their complete dynamical description involves detailed knowledge of each component and its coupling to the rest of the system. In particular, the strong coupling between transmission nodes and their fast response to changes makes its complete mathematical description too complex. One interesting aspect of such a system is that it suffers periodic disturbances at all possible scales. Some of these disturbances are so small that they only affect a few streets of a city. However, they are occasionally large enough to implicate a considerable fraction of the total U. S. power grid. A recent analysis of disturbances in the U. S. power grid [1] has shown that such disturbances are randomly distributed but that their effects [such as megawatt hours (MWh) unserved or number of customers affected] show the existence of long-range dependencies. Furthermore, the probability distribution function of the size of the disturbances has a power law scaling with the exponent close to -1. This behavior of the power transmission system is suggestive of a dynamical system close to a critical operation point [2]. In the hope of capturing some of the dynamics of transmission systems, we study here a simple network distribution model that operates close to a critical point.

The model considered here is very simple. It consists of a network of nodes. Each node represents a power generation/transmission element. The nodes are characterized by a value of a ''load,'' and they can operate up to a maximum value of the load. Each node is linked to k other nodes, its neighbors. The neighbors of a given node immediately react to any change of load of this node. The links of the network do not represent the electric grid connections. They only reflect the coupling between elements of the power transmission system. This simulates the coupling induced by the circuit equations, which are not solved in this model. In developing this model, we started with the assumption that the essential dynamics are governed by the degree of coupling of the network, how close to the maximum load each element operates, and the level of the loads transmitted when the maximum load condition is violated. For the details on how the loads are transmitted, we assume that they are of less importance to the overall dynamics and will use a random transmission to the neighboring nodes.

To represent the couplings between elements of the power system, we first consider a simple ring network; then, we increase the complexity of this network in two different ways. One way is by increasing the number of connections between nodes. This will decrease the path length but increase the clustering coefficient. The path length is defined as the shortest path between each pair of nodes averaged over all the nodes of the network. The clustering coefficient is defined as follows: for a given node we calculate the number of neighboring nodes that are connected to each other and average this number over all the nodes in the network. A second way of increasing the complexity of the network is to maintain a fixed number of connections between nodes, but to randomize them. This decreases both the path length and the clustering coefficient, although the rate of decrease is very different for these two quantities, as is typical of small-world networks [3]. Alternative two-dimensional network structures are also considered.

These different ways of increasing complexity led to very similar probability distribution functions (PDF's) of disturbances. In all cases, the PDF's have a power-scaling region with the exponent close to -1. This is consistent with the results of the analysis of disturbances of the U.S. power grid [1].

The rest of this paper is organized as follows. In Sec. II, we introduce the dynamical model for power transmission and describe the different network connections considered. The scaling of the averaged size of the disturbances with the parameters of the model is discussed in Sec. III. In Sec. IV, the resulting PDF of the disturbance size is presented, and the effect of randomization of the connections is discussed. Finally, the conclusions of the paper are given in Sec. V.

II. DYNAMICAL MODEL AND NETWORK TOPOLOGIES

A power transmission system consists essentially of three types of elements: power generators, power consumption centers, and transmission lines [4]. Because we assume that the generation matches demand, we are only concerned with generators and transmission lines. Each of these elements is characterized by a position index, I; an instantaneous load, $Z_i(t)$, at a time, t; and a critical load, Z_{crit} above which it cannot operate. In our simple model, we will take Z_{crit} to be the same for all elements of the system.

In a realistic electric grid, there is a strong coupling among all the loads in the system. This makes the calcula-

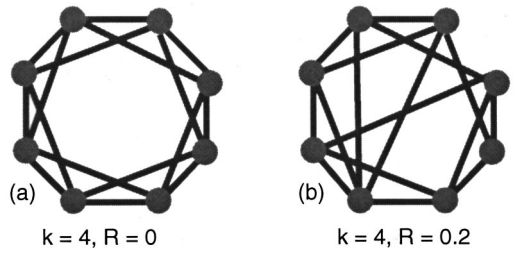

FIG. 1. Ring configuration with $L=8$ and $k=4$, where (a) the nodes are linked to their nearest neighbors ($R=0$), and (b) 20% of the links have been randomly reconnected ($R=0.2$).

tions rather complex. To avoid solving the circuit equations, we assume that this coupling may be described by defining nearest neighbors to each element. The neighbors of the element *i* are the set of other elements whose loads are most affected by a change in the load of element *i*. Therefore, we represent the coupling between elements through a network in which the elements are nodes that are linked to their neighbors. Such a network should not be confused with the electric grid itself. Let us first consider a simple configuration by assuming that the network is a ring with L nodes and that each node is connected to k of its nearest nodes, its neighbors (Fig. 1).

In the time evolution of this system, we consider two time scales. One is a time scale of the order of one day. At every daily iteration and with a probability p_0, an event may happen at node *i*. The event consists of the transfer of a unit load from (or to) *i* to (or from) one of its neighbors *j*.

$$\begin{aligned} Z_i(t+1) &\rightarrow Z_i(t) \pm 1, \\ Z_j(t+1) &\rightarrow Z_j(t) \mp 1. \end{aligned} \tag{1}$$

Here, *j* identifies the location of a randomly chosen node among the k neighbors of node *i*. We will refer to Eq. (1) as rule (1). This rule conserves the total load of the system.

At every iteration all nodes are also tested for criticality. If for any *i* $Z_i(t) > Z_{\text{crit}}$, then N_f units of load are transferred to its neighbors:

$$\begin{aligned} Z_i(t+1) &= Z_i(t) - N_f, \\ Z_j(t+1) &= Z_j(t) + n_{fj}, \end{aligned} \tag{2}$$

for all *j* neighbors of *i*. The load amounts transferred, n_{fj}, are chosen randomly with the constraint $\Sigma_j n_{fj} = N_f$. In practice, the way that it is done is as follows. Each unit load in N_f (N_f is an integer) is randomly assigned to one of the nearest *j* neighbors of *i*. As we go through each unit in N_f, more than a unit load can be assigned to the same given *j* neighbor. We will refer to Eq. (2) as rule (2). When the criticality condition for rule (2) is verified, a disturbance (avalanche) starts. At this point, we consider a change of time scale and the basic unit of time is of the order of minutes while the disturbance lasts, that is, while there are nodes with $Z_i(t) > Z_{\text{crit}}$. During this process, rule (1) is not applied. In this way the different avalanches are separated.

Both of the dynamical rules considered are conservative rules. So the averaged load per node, $\langle Z(t) \rangle$, remains constant; $\langle Z_i(t) \rangle = Z_a$. For $k=2$, this iteration scheme is equivalent to a one-dimensional sandpile with periodic boundary conditions [2]. This analogy does not hold for larger values of k. In the $k=2$ case, and because of the boundary conditions, the averaged gradient of the sandpile is constant (constant load in this model). Therefore, this system cannot self-organize. Self-organization is possible if we change rule (1) and allow the total load of the system (or gradient of the sandpile) to change with time. Nevertheless, the present model is an interesting system to study and this form of rule (1) allows us to explore its properties as the system approaches criticality. In this way, we can find out how the distribution function of avalanche sizes behaves near this point [5]. The value of Z_a controls how close to Z_{crit} the system operates. However, in practice it is better to use $\Delta Z \equiv Z_{\text{crit}} - Z_a$ as the control parameter. The other two parameters relevant to the present studies are N_f and k.

In this model, another more subtle dependence is not represented by any of the three parameters just mentioned. It is the dependence on the topology of the network. We have investigated this dependence in two different ways. One way is by randomizing the links in the network. Once we have constructed a symmetric network, we modify it in the following way. At each node *i*, we examine each of the k to the other nodes. With probability R, each link is reconnected to another randomly chosen node (Fig. 1). In choosing the new node, we exclude the nodes that have already been reconnected and, of course, we do not allow the node to be connected to itself. In this way we build a small-world network [3]. A second way of looking at the effect of the network topology is by changing the basic structure of the network. Apart from the ring structure, we have considered square, hexagon, and treelike networks (Fig. 2). For these networks the effect of the randomization of the links has also been considered.

Two parameters can be used to characterize a given network [3]. One is the path length, L_n, which can be defined as the average of the shortest paths from each node to each other node, the shortest path being the least number of links that have to be traversed to get from one node to another. The other parameter is the clustering coefficient, C. The clustering parameter of a node is defined as the number of its neighbors that are connected to each other divided by the total possible connections. The clustering coefficient is the average of the clustering parameters of all the nodes. For instance, in a ring network with $k=2n$ connection, a given node has n neighbors on its right and n neighbors on its left. Hence, on each side there are C_n^2 connections between these neighbors. Across the two groups are $n(n-1)/2$ connections. Therefore, the total number of connections between neighbors is $N_c = 3n(n-1)/2$. Since the total number of possible connections is $N_T = C_{2n}^2$, the clustering parameter is $C \equiv N_c/N_T = (3/4)(k-2)/k - 1$. For a large network, with $L \gg 1$, it is easy to see that the path length is $L_p \approx L/2k$. Therefore, in a ring network, increasing the number of connections k reduces the path length and increases the clustering parameter. The largest changes in L_n and C occur in going from $k=2$ to $k=4$. On the other hand, increasing the probability of random connections R as shown in Ref. [3] reduces both the path length and the clustering parameter, but at very different rates.

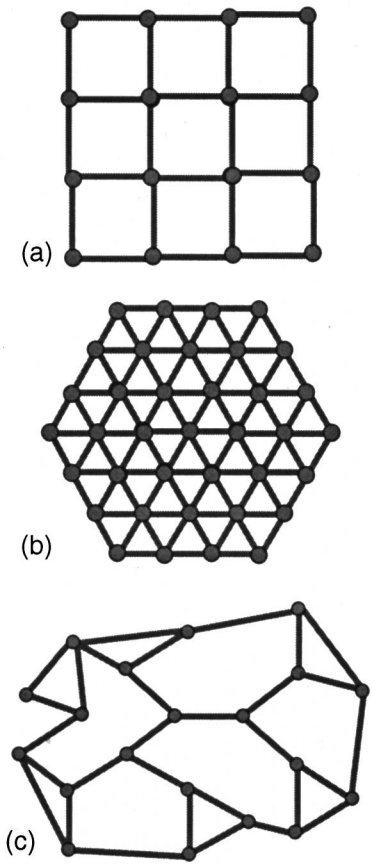

FIG. 2. Examples of networks with (a) square structure, (b) hexagonal structure, and (c) $k=3$ tree-type structure.

III. SCALING OF THE AVALANCHES

As described in the preceding section, the system evolves in such a way that avalanches cannot overlap. This seems to be a regime close to the one relevant to power distribution systems. This separation between avalanches also allows the study of their statistical properties as a function of the main parameters of the model. To do so, we consider two standard measures of the avalanches. One is the avalanche size, S, which is the total number of criticality events with forced transfer during the avalanche. Another measure is the avalanche duration, T, which is the number of iterations from the beginning of the avalanche to its end.

For most of the present studies, we have used a 200-node system, $L=200$, and $Z_{\mathrm{crit}}=105$. Because the system is closed (or, equivalently, it is like a periodic sandpile), there is no dependence of the avalanches on the size of the system. Of course, if we make the system very small, size effects can become important. There is also little dependence of the avalanches on the value of Z_{crit} while $Z_{\mathrm{crit}} \gg \Delta Z$, and $Z_{\mathrm{crit}} \gg N_f$.

We consider first a ring configuration with $R=0$; in the next section we discuss the effect of randomizing the network. Here we study the effect on the avalanches of changing ΔZ, N_f, and k. We keep two of these parameters fixed and vary the other one. In all cases studied, we have found two regimes of operation. In one regime, the avalanches are of finite size and distinctively separated. In this regime, we have found that the averaged avalanche size increases with increasing N_f and k, and with decreasing ΔZ. When we increase or decrease beyond a certain value, an avalanche can begin and travel around the network continuously. This is the second regime: nonstop avalanches. We have limited our studies to the first regime.

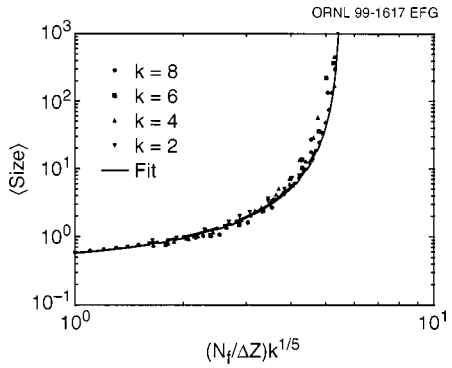

FIG. 3. Averaged avalanche size for the ring configuration as a function of $\lambda \equiv k^{\alpha} N_f/\Delta Z$, with $\alpha=0.22$. All of the data obtained varying the parameters ΔZ, k, and N_f have been included in the plot. For simplicity, we have only labeled the different k values. The continuous line is the result of fitting the data with Eq. (3).

In these studies, we have considered the following parameter ranges. The number of k connections has been varied from 2 to 12 (we only consider even values of k). For each given k, we have performed two scans in the parameter N_f, one for $\Delta Z=3$ and the other for $\Delta Z=4$. In those scans, N_f has been varied from 6 to 14. We have also performed scans with ΔZ at a fixed value of N_f and k, and for each k and $N_f=10$. In those scans, ΔZ has been varied from 3 to 8. For all of these cases, about a total of 60, avalanche data has been accumulated. We have included between 15 000 and 20 000 avalanches per case. The following results are based on the analysis of all of these cases.

All of the results of the scaling of the averaged avalanche size with the three parameters can be summarized in a single scaling in terms of the parameter $\lambda \equiv k^{\alpha} N_f/\Delta Z$. This is shown in Fig. 3 where we have plotted the averaged avalanche size for the 60 cases considered. To have all results collapsing on a single curve, $\alpha=0.22\pm0.2$. The transition between the two regimes can be expressed in terms of a threshold value for the parameter $\lambda=\lambda_0$. For the ring network configuration, $\lambda_0=5.62\pm0.26$. The uncertainty in the value of λ_0 is due to the uncertainties in the value of α. The functional dependence of the averaged avalanche size is well described by the function $\hat{S}(\lambda)$, which is defined as

$$\hat{S}(\lambda)=\frac{g_1}{(\lambda-\lambda_0)^2}, \tag{3}$$

with $g_1=12.1$. The numerical values for λ_0 and g_1 have been obtained from a fit to all data from the ring network. In Fig. 4, we compare the results from the ring network to the ones obtained using the square, hexagonal, and treelike networks. We have used the same values of L and Z_a for the ring network and $\Delta Z=3$. We have done an N_f scan for each of the three network configurations with $10 \leqslant N_f \leqslant 11$ for the square, $8 \leqslant N_f \leqslant 11$ for the hexagon, and $9 \leqslant N_f \leqslant 13$ for the treelike networks. The new data points of the averaged avalanche size fall on a curve similar to the one obtained for the ring network. As can be seen from the figure, the value of λ_0

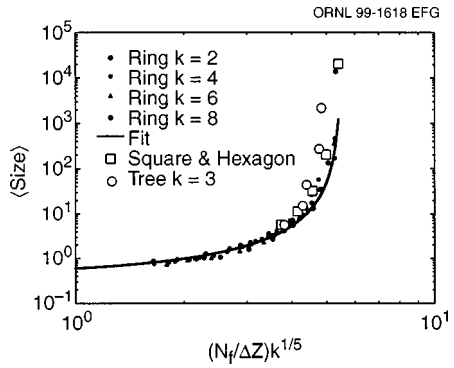

FIG. 4. Same as Fig. 3 with the addition of the data obtained using the square, hexagonal, and $k=3$ treelike networks.

for those other networks may be slightly lower than the value obtained for the ring, but the change is less than 10%. Therefore, the detailed structure of the network seems to play a very minor role in the determination of the scaling of avalanche size with λ.

Changing the number of connections k not only changes the size of the avalanches but also their topology in the space-time plane. This can be seen in Fig. 5, where we have plotted the position of a node at the time when a forced transfer occurs. In this two-dimensional plot (node position vs time), the avalanches appear as a sequence of black dots. For $k=2$, the avalanches are rather short, and most of them are represented, in this plane, by a single line. However, for $k=10$, we can see the increased complexity of the avalanche structure. A way of measuring the changes in the avalanche structure is by calculating the averaged avalanche size, $\langle S\rangle_T$, for avalanches of a given duration, T, and analyzing its dependence on T. In general, we find that it obeys a power scaling law, that is,

$$\langle S\rangle_T \propto T^{\sigma}. \tag{4}$$

Here, σ can be considered as an averaged dimension of the avalanches. When k is increased from 2 to 10, σ increases from 1.26 to 1.43 (Fig. 6).

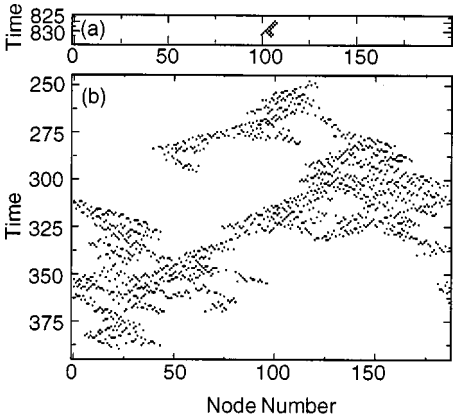

FIG. 5. Typical structure of avalanches in the plane node number-time for (a) $k=2$ and (b) $k=10$ ring configurations. Both cases are for $N_f=10$ and $\Delta Z=3$.

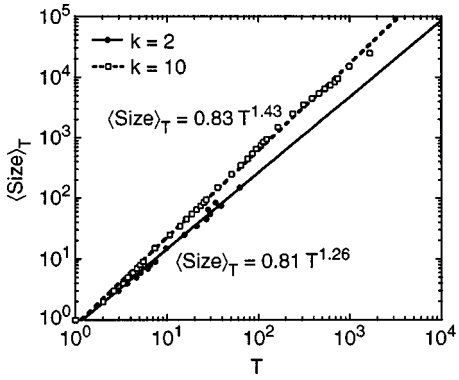

FIG. 6. Averaged avalanche size $\langle S\rangle_T$ for avalanches of a given duration T as a function of the duration T for (a) $k=2$ and (b) $k=10$ ring configurations. Same parameters as in Fig. 5.

IV. PROBABILITY DISTRIBUTION FUNCTION OF AVALANCHES

It is interesting to see how the full PDF of the avalanches changes when varying one of the three parameters of the model. For instance, in Fig. 7 we have plotted the PDF of avalanche sizes for $\Delta Z=3$, $N_f=10$, and varying k but keeping $\lambda<\lambda_0$. The PDF's are not a pure power function of S. However, there is a range of values of S for which the PDF can be approximated by a power with the exponent close to -1. As k increases, the power scaling range widens (Fig. 7). We find that the PDF of the avalanches is well described by a function of the form

$$P(S)=\frac{ge^{-S/S_0}}{1+S/S_1}. \tag{5}$$

This functional form gives a $1/S$ dependence over a broad range of scales with a cutoff at the largest scales.

For the different sets of parameters, as λ increases the value of the parameter S_0 increases faster than the value of S_1 (Fig. 8). The difference between their values is a measure of the length of the power scaling range. The same behavior is obtained by increasing λ by means of increasing k or N_f or decreasing ΔZ. In Fig. 7, we have also plotted the values of S_0 and S_1 for an N_f scan with $k=4$ and $\Delta Z=3$. As the figure shows and within the error bar due to the numerical calculations and the functional fit, both parameters in Eq. (5) can be regarded as a function of only λ.

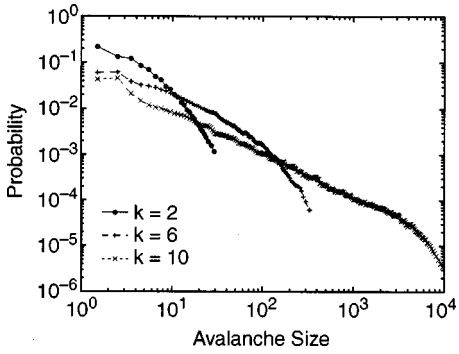

FIG. 7. PDF of avalanche size for $\Delta Z=3$, $N_f=10$, and varying k.

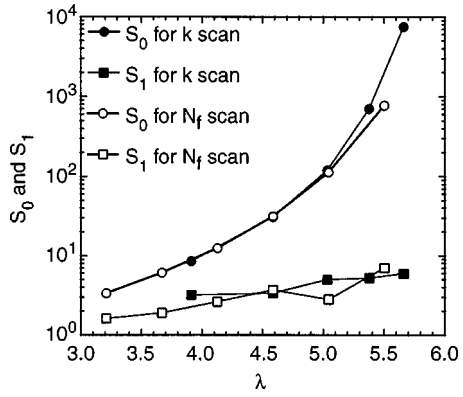

FIG. 8. Value of the parameters S_0 and S_1 for two different parameter scans. The k scan is for the same parameters as in Fig. 7. The N_f scan is for $k=4$ and $\Delta Z=3$.

The scaling of the avalanche size with N_f for the square, hexagon, and treelike networks is very similar to the scaling found for the ring network.

Note that the PDF of the different measures of the sizes of the disturbances in the U.S. power grid falls off as a power function with the exponent close to -1 [1]. In spite of the rather simple model that we have used here, the power-scaling region of the avalanches is consistent with this power dependence.

Because the parameters S_0 and S_1 are different functions of λ, there is no global self-similarity transformation of the PDF's. However, S_1 is always smaller than S_0, and in regimes of interest, $S_1 \ll S_0$. In this case, $S_0 P(S) \approx g S_1 \exp(-x)/x$, where $x=S/S_0$. This is the same as saying that a self-similarity transformation of the PDF exists for large values of S. Such self-similarity can be seen in Fig. 9, where we have plotted the PDF of the avalanche sizes for a sequence of calculations with $\Delta Z=3$, $k=4$, and varying N_f. In this figure we have plotted $S_0 P$ as a function of S/S_0. For values of $S/S_0 > 0.01$, all the data collapse onto a single curve.

Up to now, we have considered symmetric networks with $R=0$. Let us now turn to the effect of taking $R \neq 0$. Randomizing the connections in the ring networks increases the averaged avalanche size, but it is not clear that it changes the topology of avalanches. Note that the less clustered the network, the less localized an avalanche will be in the space-time plane. However, the avalanche dimensionality, as calculated in Sec. III, remains the same after randomization of the connections. The averaged avalanche size scales as a power of the clustering coefficient (Fig. 10). The change in the PDF is similar to increasing the number of connections; the power-scaling region stretches, and for low clustering coefficients, the PDF has a broad region scaling as S^{-1}. Therefore, the main effect of the randomization is to change the value of the critical point in the λ variable, decreasing the threshold to the continuous avalanche regime. For these small-world networks [3], the threshold value of the second regime is significantly decreased: $\Delta\lambda_0 \propto [C(R)/C(0)]^{0.63}$.

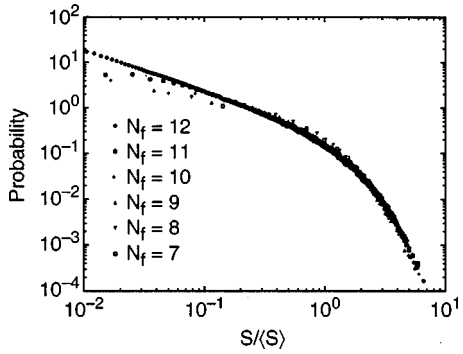

FIG. 9. PDF of the avalanche sizes for a sequence of calculations with $\Delta Z=3$, $k=4$, and varying N_f. In this figure we have plotted $S_0 P$ as a function of S/S_0.

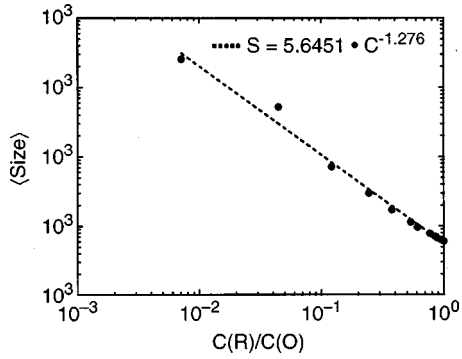

FIG. 10. Averaged avalanche size as a function of the clustering coefficient for $\Delta Z=3$, $k=4$, $N_f=10$, and varying R.

When we work at values of λ just below the threshold of the continuous avalanche regime, the calculation of the PDF becomes very difficult. In this case, some avalanches are very long, and it is difficult to obtain meaningful statistics. In this situation the functional form of the PDF is different from the one given by Eq. (5). We can see these changes better when we randomize the connection of the network because we can get as close to the threshold as we like by varying the probability R in a continuous manner. The change in the PDF is shown in Fig. 11, where we have plotted a sequence of PDF's for $\Delta Z=3$, $k=4$, $N_f=10$, and varying R.

V. CONCLUSIONS

The simple power transmission model presented here provides some insight into the nature and probability distribution of disturbances. All the results on the scaling of the averaged avalanche size with the main three parameters of the model, N_f, k, and ΔZ, can be summarized in a single

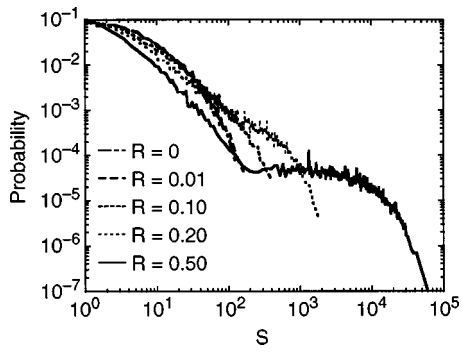

FIG. 11. PDF of the avalanche size for the same sequence of calculations as the ones shown in Fig. 10.

scaling in terms of the parameter $\lambda \equiv k^{\alpha} N_f / \Delta Z$. We have found two regimes of operation. In one regime, the avalanches are of finite size and distinctively separated. In this regime, we have found that the averaged avalanche size increases with λ. When we increase λ beyond a threshold value, λ_0, an avalanche can travel around the system indefinitely, that is, the avalanche size is infinite. This is the second regime. We have limited our studies to the first regime.

For symmetric networks, the value of the threshold does not vary significantly when we change the topology. However, λ_0 is strongly affected by randomization of the network links, small-world networks [3].

The form of the PDF seems to be rather resistant to changes in the type of connections in the system. They also have a well defined scaling form with the parameters of the model. The resistivity of the functional form of the PDF to changes in parameters and connectivity suggests that it could remain the same in more detailed models of power transmission systems. Therefore, it could come close to describing the real PDF of the disturbances. As a matter of fact, the exponent of the power-scaling region of the PDF is -1, close to the values obtained in the analysis of the disturbances in the U.S. power grid [1].

The results of this model must be tested for their relevance to real power systems. These tests require more complete models that involve the solution of the circuit equations. Work is in progress to address this issue.

ACKNOWLEDGMENTS

One of the authors (B.A.C.) gratefully acknowledges very stimulating and useful discussions with D. E. Newman and I. Dobson. This research was carried out at Oak Ridge National Laboratory, which is managed by Lockheed Martin Energy Research Corp. for the U.S. Department of Energy under Contract No. DE-AC05-96OR22464.

[1] B. A. Carreras , D. E. Newman, I. Dolrou, and A. B. Poole, in *Proceedings of Hawaii International Conference on System Sciences*, January 4–7, 2000, Maui, Hawaii.

[2] P. Bak, C. Tang, and K. Wiesenfeld, Phys. Rev. Lett. **59**, 381 (1987).

[3] D. J. Watts and S. H. Strogatz, Nature (London) **393**, 440 (1998).

[4] A. R. Bergen, *Power System Analysis* (Prentice-Hall, Upper Saddle River, NJ, 1970).

[5] R. Dickman, A. Vespignani, and S. Zapperi, Phys. Rev. E **57**, 5095 (1998).